Macromolecules

Article

pubs.acs.org/Macromolecules

Intercrystalline Links Determined Kinetics of Form II to I Polymorphic Transition in Polybutene-1

Yongna Qiao[†,‡] and Yongfeng Men*[,†,‡]

[†]State Key Laboratory of Polymer Physics and Chemistry, Changchun Institute of Applied Chemistry, Chinese Academy of Sciences, Renmin Street 5625, Changchun 130022, P. R. China

[‡]University of Science and Technology of China, Hefei 230026, P. R. China

Supporting Information

ABSTRACT: The effect of intercrystalline links containing tie molecules and entangled loops on polymorphic transition from form II to form I in polybutene-1 (PB-1) of different molecular weights has been investigated by differential scanning calorimetry and small-angle X-ray scattering techniques. The PB-1 samples were isothermally crystallized at a range of temperatures to develop metastable form II crystalline modification of different lamellar thickness, long spacing, and number of intercrystalline links in the amorphous phase. Tammann's two-stage crystal nuclei development method was applied to promote a faster polymorphic transition from form II to I; that is, form I nuclei were developed at the early low temperature stage, and form I crystals were formed at the later high temperature stage. At a given annealing condition, the transition rate in the high molecular weight sample is found to increase with the increase of the prior form II crystallization temperature, while it shows a negative correlation between transition rate and crystallization temperature in the low molecular weight sample. The results can be understood as follows. The long spacing of high molecular weight PB-1 is smaller than the radius of gyration of the chains in the melt, leading to formation of folded-chain crystals and high possibility of generating intercrystalline links. Higher internal stress induced by unbalanced shrinkage of amorphous and crystalline phases would be built up during cooling from higher crystallization temperature to the first temperature stage of annealing. For low molecular weight samples, the probability of forming intercrystalline links decreases with the increasing lamellar thickness at elevated crystallization temperature. For a low crystallization temperature where intercrystalline links could be found in both samples, the low molecular weight sample shows a faster transition for its higher chain mobility. These molecular mechanisms are discussed in this article.

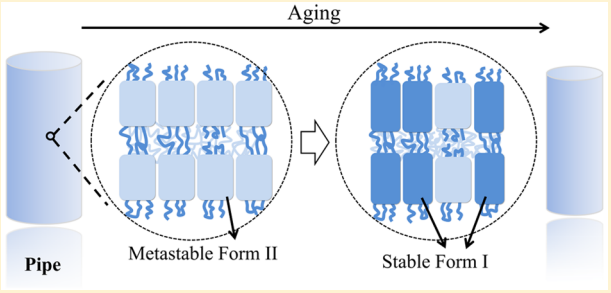

INTRODUCTION

Synthetic polymers with linear architectures and regular chemical constitutions exhibited the potential to crystallize.[1] Lamellar structures might be formed when polymer melt was cooled to temperatures below the equilibrium melting point. Crystallization of semicrystalline polymer was a kinetically controlled process, and the lamellar thickness highly depended on the supercooling,[2,3] which showed a positive correlation with crystallization temperature, T_c.[4,5] Lamellar structures were separated by disordered amorphous region, which was constituted of entanglements, end groups, tie molecules, and short chain branches. Tie molecules were referred to the molecules that participated in growth of two or more adjacent lamellae which would reinforce the aggregate structure.[6] Such intercrystalline links play a prime role in the mechanical properties via stress transmission.[7,8] Lamellar growth continued until tie molecules were pulled taut.[9] However, tie molecules will probably be formed only when the molecules have an end-to-end distance in the melt equal to or larger than the distance between adjacent crystallites.[10] There were only a few relatively short tie chains in low molecular weight (MW) polymer, while the number of ties was increased in higher molecular weight samples, the conformation of which changed from extended-chain conformation to folded-chain crystallites.[11−13]

Isotactic polybutene-1 (PB-1) has attracted a great deal of industrial interest due to its outstanding mechanical properties, such as its superior creep resistance, hardness, and stiffness.[14] PB-1 is a typically polymorphic semicrystalline polymer, which exhibited four different crystalline modifications: I, II, III, and I′.[14−19] But only the tetragonal form II with an 11/3 helix[20] and hexagonal form I with a 3/1 helical conformation[21] were focused in this paper due to their practical significance in industry. PB-1 usually forms the kinetically favored form II crystal, which is metastable, when it is crystallized from melt. Form II crystals slowly transform into the thermodynamically stable form I crystals spontaneously and irreversibly with an enhancement of mechanical properties and melting points,[22] when the sample is stored at room temperature. A remarkable

Received: April 13, 2017
Revised: July 2, 2017
Published: July 13, 2017

DOI: 10.1021/acs.macromol.7b00771
Macromolecules 2017, 50, 5490−5497

volumetric change or deformation of the PB-1 could be observed when it was in storage at room temperature, which was ascribed to the difference in unit cell size and shape between forms II and I.[23,24] It needs several weeks to complete the form II to I polymorphic transition. In order to overcome such a practical problem, many investigations have been conducted to shorten the transition time. It was found that the phase transition could be greatly accelerated by external and thermal stress,[25−28] high pressure,[21,29] pressured CO_2,[30−32] solvent annealing,[33] and copolymerization with random 1-alkane counits fewer than five carbons.[34] Recently, a new temperature program was conducted by us to significantly shorten the transition time, which decomposed the phase transition into nucleation and growth by employing Tammann's two-stage crystal nuclei development method on crystal-to-crystal phase transition in PB-1.[35] It has been reported that the form II to I transformation in PB-1was a nucleation-controlled process.[36−38] Quenching the form II crystals immediately after isothermal crystallization to a low temperature near the glass transition temperature (T_g) made the nucleation of form I within form II crystals easier because of the greater thermodynamic driving force, the smaller critical cluster size, and the internal stress built up during cooling from the higher isothermal crystallization temperature. After the nucleating procedure at low temperature, the following annealing at higher temperature provided a high growth rate of the predeveloped nuclei.

The structures of crystalline and amorphous region in polymer are strongly related to the molecular weight and crystallization temperature,[13] which will further influence the nucleation and growth behaviors in polymorphic transition due to the difference of intercrystalline links and chain mobility. In our previous work, the optimal nucleation temperature in the form II to form I transition was found to be about −10 °C, and the fastest growth occurred at 40 °C.[35] Besides, a positive correlation between the phase transition degree and crystallization temperature of form II was found in the PB-1 samples. Therefore, in this work, the influence of morphology and structure on the form II to I phase transition in PB-1 was explored by investigating the phase transition behaviors of PB-1 samples with different molecular weights and crystallized at different temperatures. Lamellar thickness and long spacing that characterize the aggregate structure in polymer were determined by means of small-angle X-ray scattering (SAXS) techniques. In particular, the SAXS pattern of PB-1 form II can hardly be detected at room temperature because the electron density of PB-1 crystalline form II (0.89 g/cm^3) is similar to the amorphous phase (0.87 g/cm^3).[20,39] Thus, the lamellar thickness and long spacing of PB-1 samples were determined immediately after the form II crystallization at the corresponding crystallization temperature at which the amorphous phase expanded to a greater degree than the crystalline phase; thus, the electron density difference was increased, and the scattering signal could be relatively higher and detectable.[13] Synchrotron SAXS measurement was employed to determine the lamellar thickness and long spacing of PB-1 samples of different molecular weights crystallized at different temperatures. By means of differential scanning calorimetry (DSC), the content of form I was obtained after partially transformation of the form II crystallites by annealing at the optimal temperatures of nucleation and growth successively.

EXPERIMENTAL SECTION

The three PB-1 samples with different molecular weights were produced by LyondellBasell, the physical properties of which are given in Table 1. The crystallinity of PB-1 samples after isothermal crystallization was determined by DSC and shown in Table 1. The crystallinity value varies due to different crystallization temperatures from 50 to 95 °C. For Gaussian chains, the radius of gyration is an estimate of the diameter of the volume occupied by the chains in the melt and can be obtained as follows:

Table 1. Characterization of PB-1 Samples

trade name	melt flow rate (MFR) (190 °C/2.16 kg)	M_w (kg/mol)	crystallinity Φ_w	R_g (nm)	PDI
PB0110	0.4	711	0.54−0.71	42.4	3.5
PB0400	16.4	188	0.60−0.73	21.9	2.7
PB0800	200.0	77	0.66−0.78	14.0	3.0

$$R_g^2 = \frac{R_0^2}{6}$$

where R_0 is the mean-squared end-to-end distance and can be calculated via the characteristic ratio C_∞ as

$$R_0^2 = C_\infty a_b^2 N$$

where a_b^2 represents the sum of the squares of the lengths of the backbone bonds of one monomer unit and N is the degree of polymerization. For PB-1, C_∞ is 18 and a_b^2 is 4.74×10^{-2} nm^2.[40] The radius of gyration of each PB-1 sample is also listed in Table 1.

PB-1 samples were compression-molded into films of about 0.5 mm in thickness at 180 °C and held in molten state for 5 min to erase the processing history. The molten films were transferred rapidly into isothermal water bath at different preset temperatures and held isothermally for 2 h (T_c = 50, 60, 70, and 80 °C) or 5 h (T_c = 85, 90, and 95 °C) to complete the crystallization.

In order to describe the lamellar thickness of the isothermally crystallized PB-1 samples with different MWs, synchrotron SAXS measurements were performed at the corresponding crystallization temperature at beamline BL16B1 at SSRF, Shanghai, China.[41] The wavelength of the X-ray radiation was 0.124 nm, and the distance of the sample-to-detector was 1880 mm. Each SAXS pattern obtained in the center of the sample was collected within 60 s, which was then background corrected and normalized using the standard procedure. The scattering patterns after calibration were averaged over all directions at a constant scattering vector, $\mathbf{q}$, resulting in one-dimensional scattering intensity curves. Because of the isotropic distributed stacks of parallel lamellar crystallites in the system, Lorentz correction(multiplication of I by q^2) was performed in order to calculate the long spacing of the lamellar stacks. Structural parameters (d_{ac}, d_c, and d_a) of the samples in form II were obtained via correlation function approach, where d_{ac}, d_c, and d_a denote the long spacing, lamellar thickness, and thickness of amorphous phase, respectively.[42] The electron density correlation function $K(z)$ can be derived from the inverse Fourier transformation of the experimental intensity distribution $I(q)$ as follows:[42−44]

$$K(z) = \frac{\int_0^\infty I(q) q^2 \cos(qz)\, dq}{\int_0^\infty I(q) q^2\, dq} \quad (1)$$

where z denotes the location measured along a trajectory normal to the lamellar surfaces, and the multiplication of $I(q)$ with q^2(Lorentz correction) was performed. For systems with a structure of stacks of lamellae, the correlation function shows characteristic features that allow the long spacing defined as the average thickness of a lamella together with one interlamellar amorphous layer measured along the lamellar normal to be determined.

DOI: 10.1021/acs.macromol.7b00771
Macromolecules 2017, 50, 5490−5497

Thermal analyses were conducted with a DSC1 Star^e System (Mettler Toledo Instruments, Swiss) under a nitrogen atmosphere (50 mL/min). The instrument was calibrated with high purity indium as a standard to ensure reliability of the data required. The main thermal protocols are presented in the top of Figure 1. After melting at 160 °C for 8 min to erase the thermal history, PB-1 melts were rapidly cooled to T_c and held for 30 or 60 min (T_c = 95 °C) for the complete crystallization of form II. Then, form II obtained from different T_c was annealed at −10 °C for a 60 min nucleation followed by annealing at 40 °C for a 220 min growth of form I crystals. The cooling and heating rates in processes from T_c to −10 °C and then to 40 °C are both 50 K/min. The annealed samples were heated to 160 °C at a rate of 20 K/min to obtain the melting curve, from which the contents of forms II and I were obtained via melting peak fitting and integrating procedure considering exponentially modified Gaussian functions as was shown in the bottom part of Figure 1.[45,46] The melting ranges of forms II and I are around 115−120 and 125−130 °C, respectively. The degree of the phase transition can be manifested as the content of continuous transformed form I:

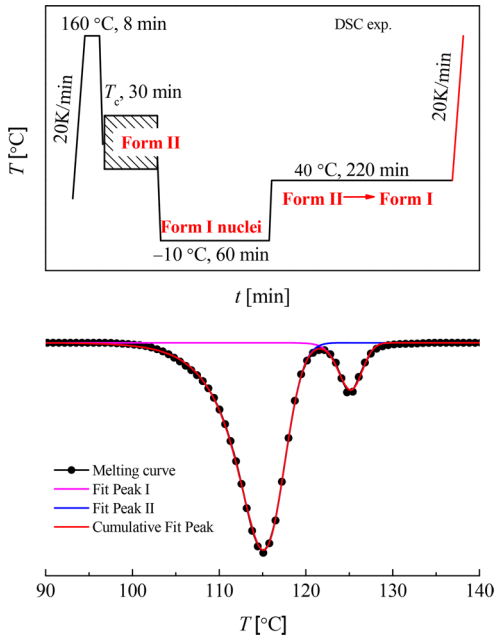

Figure 1. Schematic illustration of dynamic thermal treatment applied to PB-1 samples (top), and examples of multiple peak fitting analysis of DSC melting curves obtained from the last heating process in top figure, to decompose the melting process of form I and form II crystallites in the 95 °C crystallized PB0800 sample.

$$X_I = \frac{A_I/\Delta H_{id,I}}{A_I/\Delta H_{id,I} + A_{II}/\Delta H_{id,II}} \quad (2)$$

where A_I and A_{II} are the areas of form I and form II melting peaks; $\Delta H_{id,I}$ and $\Delta H_{id,II}$ are the melting enthalpy of ideal crystals in form I and form II, which are 141 and 62 J g^{-1},[47] respectively.

RESULTS AND DISCUSSION

It is well-known that the structure of polymers strongly depends on the crystallization condition. Figure 2 shows the Lorentz corrected one-dimensional scattering intensity distributions of the three PB-1 samples crystallized at a series of T_c ranging from 50 to 95 °C. The first- and second-order scatterings were observed in a wide range of crystallization temperatures from 50 to 95 °C. The scattering peaks moved to smaller q with the increase of the crystallization temperature in all the three samples, indicating an increase of the d_{ac}. Values of

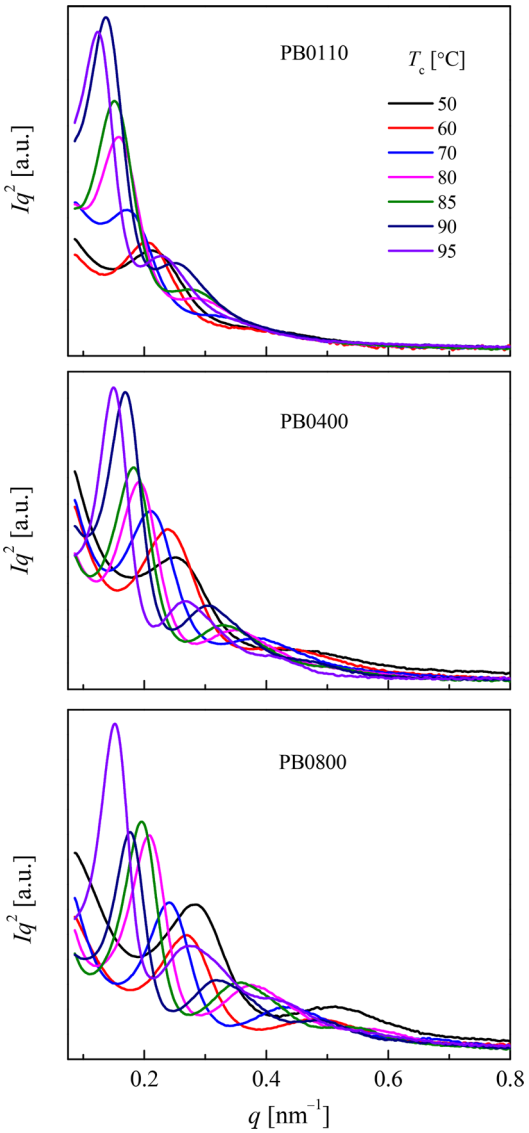

Figure 2. Selected one-dimensional scattering intensity distribution profiles of form II crystals of PB0110 (top), PB0400 (middle), and PB0800 (bottom) samples after being isothermally crystallized at different temperatures from the homogeneous melts.

the thicknesses of crystalline lamellae (d_c), the amorphous layers (d_a), and the long spacing (d_{ac}) of PB-1 samples in form II crystalline structure were derived from the correlation function approach, which are listed in Table 2. Because of the crystallinity of each sample was larger than 50%, the smaller value obtained from the intersection point of the correlation function was assigned to d_a, and d_c was obtained by the equation $d_c = d_{ac} - d_a$.

It was verified in our previous work that the form II to I phase transition in PB-1 was a two-step process, including nucleation and growth.[35] The nucleation process proceeded during the early stage annealing at low temperature near T_g, and the growth occurred in the late stage annealing at high temperature around 40 °C. In DSC run, three PB-1 samples were first isothermally crystallized at a series of temperatures from 50 to 95 °C from the homogeneous melt, annealed at −10 °C for 60 min and at 40 °C for 220 min, and heated up to 160 °C finally to obtain the melting curves after the partial phase transition from form II to form I. Figure 3 shows the melting

DOI: 10.1021/acs.macromol.7b00771
Macromolecules 2017, 50, 5490−5497

Table 2. Values of Lamellar Thickness (d_c) and Long Spacing (d_{ac}) of Form II Crystals in Three PB-1 Samples after Being Isothermally Crystallized at Different Temperatures

	PB0110		PB0400		PB0800	
T_c/°C	d_c/nm	d_{ac}/nm	d_c/nm	d_{ac}/nm	d_c/nm	d_{ac}/nm
50	15.9	27.7	14.1	24.6	12.7	22.3
60	16.7	28.9	14.7	25.4	13.4	23.5
70	19.6	34.2	16.8	29.1	15.0	26.3
80	21.6	37.3	18.4	32.1	17.4	30.4
85	22.6	39.1	19.4	33.8	18.5	32.1
90	25.1	43.8	21.0	36.9	20.4	35.6
95	27.8	48.5	23.7	41.1	23.5	41.0

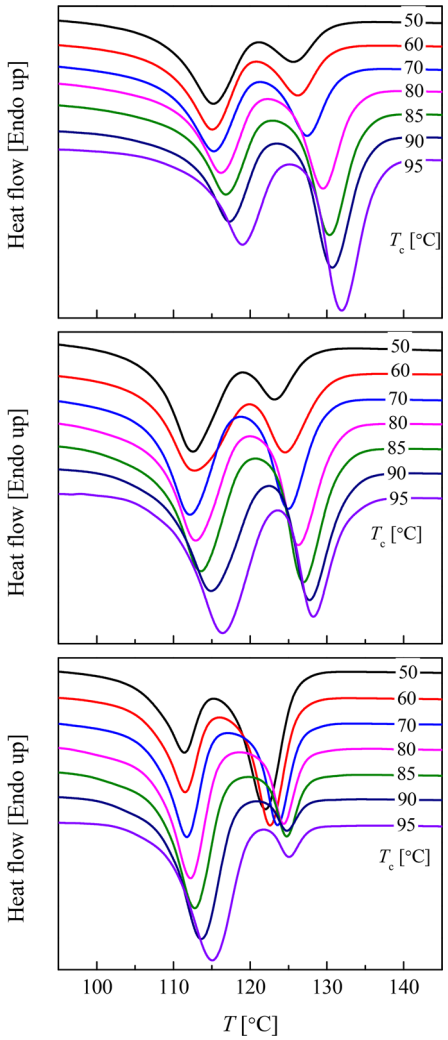

Figure 3. DSC melting curves of PB0110 (top), PB0400 (middle), and PB0800 (bottom) samples annealed at 40 °C for 220 min with a prenucleation at −10 °C for 60 min, after being isothermally crystallized at different temperatures as indicated in the figure.

process of the three PB-1 samples obtained after the partial form II to I phase transition. The metastable form II melted at lower temperature at around 115 °C, and the melting peak of stable form I appeared at about 125 °C. In the top part, PB0110 seemed to develop an increasing amount of form I with the increase of crystallization temperature at a certain annealing condition, indicating an enhancement of transition rate. The rapid cooling from higher crystallization temperature to the low annealing temperature where nucleation of form I occurs results in a larger shrinkage in amorphous phase, compared to the form II crystalline phase, due to the difference of thermal expansion coefficient between form II crystals and amorphous phase, which would introduce strong internal stress along the normal of crystalline lamellae via intercrystalline links such as chain entanglements and tie molecules. The DSC melting curves of the middle molecular weight sample PB0400 that underwent stepwise annealing are shown in the middle part of Figure 3. Melting peak areas of the form II and I in PB0400 changed nonmonotonically with the increase of crystallization temperature. But the melting peak area of form I decreased monotonically as the crystallization temperature was increased in low MW PB0800 as illustrated in the bottom of Figure 3, which was completely contrary to the case of PB0110. Figure 4

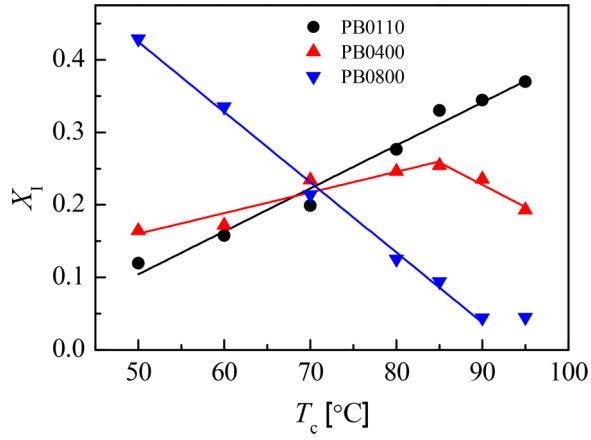

Figure 4. Fraction of form I crystals formed in each PB-1 sample after the partially form II to I phase transition at the same stepwise annealing condition against the isothermal crystallization temperature derived from the DSC melting curves in Figure 3.

depicts the fraction of form I crystals formed in each PB-1 sample after the partial form II to I phase transition at the same stepwise annealing condition of the three samples against the isothermal crystallization temperature derived from the DSC melting curves in Figure 3. One could see that the transition degree (X_I) of high MW PB0110 and low MW PB0800 showed linear but opposite dependency on crystallization temperature. Interestingly, for medium MW PB0400, the change of X_I exhibited a similar tendency to PB0110 at relatively low temperature region (at 50−85 °C) but became more analogous to the case of PB0800 at the high temperature region (at 85−95 °C).

It has been found that the rate-determining step in the PB-1 form II to I phase transition is the nucleation process, which could be strongly enhanced by thermal or internal stress.[25,36] Intercrystalline links containing chain entanglements and tie molecules are essential to the stress transmission. The intercrystalline links were supposed to be initiated by molecular chains that contact the surfaces of two or more different crystallites, which have been found in increasing amount with the increase of molecular weight.[9] It was assumed by Fu et al. that chain disentangling was not necessary during crystallization if the crystal thickness was smaller than the chain dimensions in the melt, and the entanglements could be shifted into amorphous regions.[11] In Fischer's solidification model for semicrystalline polymers, it was assumed that the random coil

DOI: 10.1021/acs.macromol.7b00771
Macromolecules 2017, 50, 5490−5497

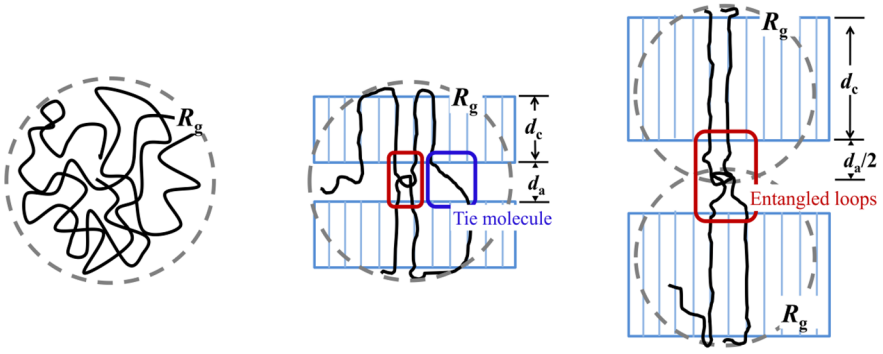

Figure 5. Sketch of chain dimensions in the melt (a) and two situations after crystallization for amorphous chain segments with a radius of gyration R_g equal to $d_c + d_a/2$ (b) or $(d_c + d_a/2)/2$ (c).

conformation in the melt was roughly preserved through crystallization, and only local rearrangements of chain segments into parallel stems were allowed for the growth of crystalline lamellae.[48] The chain dimensions in the melt can be estimated by the radius of gyration R_g, as shown in Figure 5a. The condition for crystallization without disentanglement to form both entangled loops and tie molecules could be derived as follows (Figure 5b):

$$d_c + d_a/2 \,[[\text{mml:lt}]]\, R_g \tag{3}$$

It has been found that the global conformation of a single chain is preserved upon rapid crystallization; namely, the radius of gyration, R_g, has almost the same value before and after crystallization from the SANS data analysis.[49,50] The single molecule must be incorporated into several lamellae when the radius of gyration of the chain is large enough. It is reasonable to compare the value of R_g and structural parameters after crystallization. The chains need to partially disentangle to crystallize into extended-chain crystals and unable to form tie molecules if the thickness of lamellar and a half amorphous phase is larger than R_g. The R_g values of the three PB-1 samples were calculated according to their weight-averaged MW as shown in Table 1. But there is still probability to build up intercrystalline links as entangled loops when the value of $d_c + d_a/2$ is smaller than $2R_g$, as the situation illustrated in Figure 5c.

The relationship between the ratio of $d_c + d_a/2$ to R_g of form II crystallites in the three PB-1 samples and crystallization temperatures is plotted in Figure 6. The ratio increased with the increasing T_c, as the lamellar thickness and long spacing increased. For the high MW PB0110 sample, the ratio is always smaller than 1; thus, both tie molecules and entangled loops would be formed when it was crystallized in the whole temperature range studied here. However, the ratio in PB0800 was always above 1 and becomes larger than 2 when crystallization temperature increased to 95 °C, where almost no entangled loops and tie molecules could be built up. The probability of forming entangled loops tends to be lower with the increasing value of the ratio. For PB0400, in the low T_c region below 70 °C, the thicknesses of lamellar and amorphous phase were relatively small that chain segments are long enough to generate intercrystalline links, and the ratio of $d_c + d_a/2$ to R_g was less than 1 accordingly. In the high T_c region of 80−95 °C, the ratio in PB0400 is between 1 and 2, indicating that there is less chance to find tie molecules but still the possibility of the

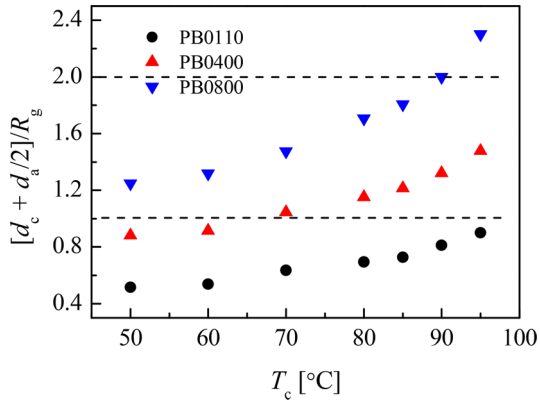

Figure 6. Ratio of $d_c + d_a/2$ to R_g of form II crystallites in the three PB-1 samples as a function of crystallization temperature.

generation of entangled loops constructed by two adjacent chains.

For low MW PB0800, according to the results in Figure 6, the chains were relatively short for forming tie molecules which occurs only when R_g is larger than $d_c + d_a/2$. As the crystallization temperature increased from 50 to 95 °C, the ratio of $d_c + d_a/2$ to R_g increased from 1.2 to 2.1. It became more difficult to keep the entanglement in loops between two neighboring lamellae as the ratio approached to 2. Consequently, the probability of generating intercrystalline links decreased with the increase of T_c over the temperature region of 50−95 °C; thus, the available nucleation site where the intercrystalline links transmitted internal stress diminished. The nucleation density decreased as the T_c was increased even though the internal stress between amorphous and form II crystalline phases was enhanced when PB-1 melt was cooled from crystallization stage to low temperature nucleation stage. The internal stress was introduced by the difference in thermal expansion coefficients of PB-1 amorphous and form II crystalline regions.[35] As a result, the X_I showed a negative correlation with T_c in PB0800.

For medium MW PB0400, lamellae tended to be thicker as the crystallization temperature was increased from 50 to 95 °C, and the ratio of $d_c + d_a/2$ to R_g increased from 0.8 to 1.4. When crystallized at relatively low temperatures (at 50−70 °C), a majority of chains were long enough to form chain-folded crystals, and the number of intercrystalline links was less influenced by the increase of T_c and d_c. However, the internal

DOI: 10.1021/acs.macromol.7b00771
Macromolecules 2017, 50, 5490−5497

stress was effectively enhanced because of the larger temperature difference during cooling from higher T_c to the low annealing temperature, which benefits the generation of form I nuclei. Therefore, X_I for PB0400 that underwent the same annealing process increased with the increasing T_c, which was analogous to the high MW PB0110.The crystallization mechanism started to change from folded-chain to extended-chain crystallization when $d_c + d_a/2$ became larger than R_g above 70 °C, where it was difficult to find tie molecules but still a chance to find entangled loops connecting adjacent lamellae. Considering the wide MW distribution of the industrial PB-1 products, about 2.5−3.5 (listed in Table 1), there are still a small number of tie molecules formed by the long chain fraction when $d_c + d_a/2$ becomes slightly larger than R_g. But the tie molecules are less likely to form as the crystal thickness was increased due to the limited content of long chain fraction in PB-1 polymer. Thus, the X_I keeps the positive correlation with T_c until 85 °C even though the ratio of $d_c + d_a/2$ to R_g is slightly larger than 1 at T_c above 70 °C. At T_c = 85 °C, the ratio of $d_c + d_a/2$ to R_g in PB0400 crystallized at 85 °C is almost equal to the ratio in PB0800 crystallized at 50 °C. The situation for PB0400 crystallized at higher T_c (above 85 °C) is similar to the PB0800 that crystallized at the temperature above 50 °C—that the transition degree after the same annealing condition decreased with the increasing crystallization temperature for lack of intercrystalline links.

It was also seen from Figure 4 that there were obviously different contents of form I formed after phase transition in the same annealing condition when the three PB-1 samples were crystallized at 50 and 95 °C. At T_c = 50 °C, folded-chain crystals formed in all three samples with enough intercrystalline links to transfer stress for nucleation as the $d_c + d_a/2$ were smaller or slightly larger than R_g. The X_I of PB0800 is larger than PB0110, which means the PB-1 form II to I phase transition shows a higher rate for the low MW sample. The factor that governed the transition rate was considered to be the chain mobility that affected the growth rate during annealing at 40 °C. The growth rate is controlled by thermodynamic driving force and free energy of activation for short-range diffusion of segments across the interface to join a lattice.[51] Since the supercoolings were equal for the three samples at 50 °C, the crystal growth rate was only controlled by the diffusion rate. As pointed out by Cheng, the chain mobility on the crystal surface was strongly dependent on the MW and mobility within the chain increases from center to the ends.[52] At T_c = 95 °C, more form I crystals were developed in high MW PB0110 sample, which was related to the higher tie molecule densities. Only a tiny amount of entangled loops could be found in low MW PB0800 when the crystal thickness was much larger than its R_g. PB0400 had a shorter chain length and similar $d_c + d_a/2$ value with R_g, which lead to fewer tie molecules compared with PB0110. At T_c = 70 °C, the contents of form I crystals are nearly the same for the three PB-1 samples, at which the internal stress induced by shrinkage of amorphous phase during cooling was similar. Although the chain mobility decreased with the increase of the MW, the number of tie molecules increased. As a result, three PB-1 samples showed similar transition rate at T_c = 70 °C. After varying nucleation/growth times for PB-1 samples with different MW crystallized at the same temperature, it showed that the molecular weight and intercrystalline linkages are affecting both nucleation and growth (see Figures S1 and S2 in the Supporting Information).

The results in Figure 4 exhibited the cooperative effects of number of intercrystalline links, internal stress induced by different shrinkage between amorphous and form II phase during cooling from T_c to low annealing temperature, and chain mobility on the PB-1 form II to I phase transition. These factors were under the control of the crystallization temperature and molecular weight and further affect the nucleation and growth rate in phase transition. The enhancement of form II to I phase transition in butene-1 copolymers might be further understood by taking into account information obtained in this work. As the rate of form II to I transition is first of all related to the thermodynamic stability of form I and form II, such enhanced phase transition in copolymers can be considered as a result of the influence of the thermodynamic stability of both form II and form I crystallites in the copolymers by the presence of constitutional defects (comonomers). In addition, when samples were cooled from crystallization to annealing temperature, the greater amounts of intercrystalline links in copolymers introduced more nucleation sites via stress transmission and further accelerated the overall transition rate.

The phase behavior during melting, crystallization, and polymorphic transition of PB-1 samples with different MWs and at various T_cs is schematically illustrated in Figure 7. When

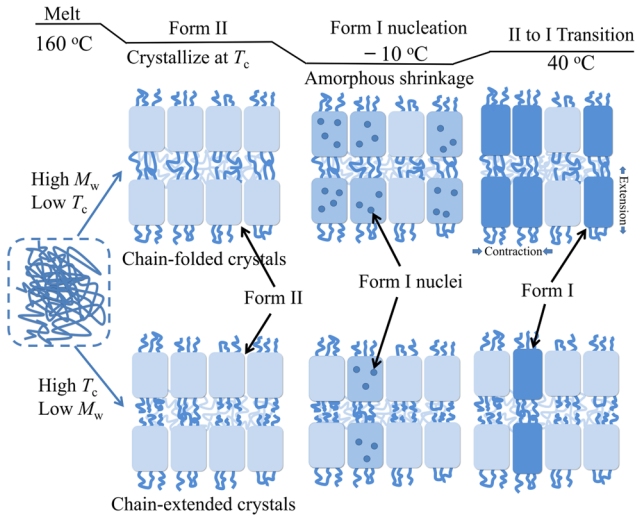

Figure 7. Schematic diagram of the phase behavior during melting, crystallization, and polymorphic transition of PB-1 samples with different molecular weights and at various T_cs.

PB-1 melt was cooled to T_c rapidly, folded-chain crystals with high tie molecule densities were usually formed in the samples with high MW or crystallized at low T_c. By means of Tammann's two-stage crystal nuclei development approach, three PB-1 samples were cooled down to −10 °C after the completion of crystallization. In the cooling process, the bigger shrinkage in amorphous phase induced the internal stress along the normal direction of lamellae which promoted the chain slippage and chain conformation transformation from 11/3 to 3/1, making the nucleation of form I easier. It was found by Miyoshi et al. that the crystalline stems in metastable form II performed uniaxial rotational diffusion accompanying side chain conformational transitions while the crystalline stems and side chain conformations were completely fixed in form I crystals up to melting points.[53,54] Large undercooling at low temperature led to the increase of the nucleation driving force and the decrease of the critical nucleus size, resulting in a fast

DOI: 10.1021/acs.macromol.7b00771
Macromolecules 2017, 50, 5490−5497

nucleation and a higher nucleation density. Therefore, these prenucleated samples showed a high growth rate on the nuclei formed at low temperature after being heated up to 40 °C. However, samples with low MW or crystallized at high temperature, which had a larger d_c than R_g, were likely to disentangle to develop extended-chain crystals, but less capable of forming tie molecules as illustrated in the bottom part of Figure 7. In this situation, internal stress could not be introduced in the "isolated" crystalline lamellae; thus, fewer sites were available to nucleation, leading to a low nucleation density in the low temperature annealing stage. When the low MW PB-1 samples were heated up to 40 °C, at which the nucleation ability was limited, the growth of form I crystals occurred slowly. In this case, intercrystalline links became a crucial factor for nucleation in the crystal-to-crystal phase transition, during which the nucleation was the most time-consuming step. Moreover, chain mobility played a vital role when there were enough intercrystalline links for sufficient nucleation.

CONCLUSION

In summary, we have investigated the molecular weight dependency of phase transition behavior of PB-1 crystallized at different temperatures using DSC and SAXS techniques. It showed different relationships in phase transition degree−crystallization temperature profiles after annealing at the same conditions for different molecular weight samples. It found a positive correlation between transition degree and crystallization temperature in high molecular weight sample but a negative correlation in the low molecular weight one. The radius of gyration R_g in high MW PB-1 samples is large enough to form folded-chain crystals and intercrystalline links, which transmitted the internal stress induced by the unbalanced shrinkage of amorphous and crystalline phase because of their different thermal expansion coefficients during cooling to crystalline phase, which would benefits nucleation of the new form I crystals. Such internal stress would be enhanced with the increase of crystallization temperature, which leads to a larger temperature range between crystallization stage and nucleation stage. In the low molecular weight sample, the thickness of lamellae and a half amorphous phase starts to be larger than R_g, and the number of intercrystalline links diminished as the crystallization temperature increased. A correlation between number of intercrystalline links and phase transition is thus established.

ASSOCIATED CONTENT

Supporting Information

The Supporting Information is available free of charge on the ACS Publications website at DOI: 10.1021/acs.macromol.7b00771.

Transition degree−nucleation/growth time profiles of isothermally crystallized PB-1 samples (PDF)

AUTHOR INFORMATION

Corresponding Author

*E-mail: men@ciac.ac.cn (Y.M.).

ORCID

Yongfeng Men: 0000-0003-3277-2227

Notes

The authors declare no competing financial interest.

ACKNOWLEDGMENTS

This work is supported by the National Natural Science Foundation of China (21134006, 51525305) and SSRF project (Z15sr0043). We thank Dr. Jinyou Lin at SSRF for assistances during synchrotron X-ray scattering experiments and Dr. Hai Wang in our group for proofreading the text.

REFERENCES

(1) Strobl, G. The Semicrystalline State. In *The Physics of Polymers: Concepts for Understanding Their Structures and Behavior*; Springer: Berlin, 2007; pp 165−222.

(2) Hoffman, J. D.; Miller, R. L. Kinetics of Crystallization from the Melt and Chain Folding in Polyethylene Fractions Revisited: Theory and Experiment. *Polymer* **1997**, *38* (13), 3151−3212.

(3) Hu, W. B. *Principles of Polymer Crystallization*; Chemical Industry Press: Beijing, 2013.

(4) Kawai, T.; Keller, A. On the Density of Polyethylene Single Crystals. *Philos. Mag.* **1963**, *8* (91), 1203−1210.

(5) Roe, R. J.; Bair, H. E. Thermodynamic Study of Fold Surfaces of Polyethylene Single Crystals. *Macromolecules* **1970**, *3* (4), 454−458.

(6) Bassett, D. C.; Keller, A.; Mitsuhashi, S. New Features in Polymer Crystal Growth from Concentrated Solutions. *J. Polym. Sci., Part A: Gen. Pap.* **1963**, *1* (2), 763−788.

(7) Séguéla, R. Critical Review of the Molecular Topology of Semicrystalline Polymers: The Origin and Assessment of Intercrystalline Tie Molecules and Chain Entanglements. *J. Polym. Sci., Part B: Polym. Phys.* **2005**, *43* (14), 1729−1748.

(8) Keith, H. D.; Padden, F. J.; Vadimsky, R. G. Intercrystalline Links in Polyethylene Crystallized from the Melt. *J. Polym. Sci., Part A-2: Polym. Phys.* **1966**, *4* (2), 267−281.

(9) Keith, H. D.; Padden, F. J., Jr.; Vadimsky, R. G. Intercrystalline Links in Bulk Polyethylene. *Science* **1965**, *150* (3699), 1026−1027.

(10) Fischer, E. W.; Hahn, K.; Kugler, J.; Struth, U.; Born, R.; Stamm, M. An Estimation of the Number of Tie Molecules in Semicrystalline Polymers by Means of Neutron-Scattering. *J. Polym. Sci., Polym. Phys. Ed.* **1984**, *22* (8), 1491−1513.

(11) Fu, Q.; Heck, B.; Strobl, G.; Thomann, Y. A Temperature- and Molar Mass-Dependent Change in the Crystallization Mechanism of Poly(1-butene): Transition from Chain-Folded to Chain-Extended Crystallization? *Macromolecules* **2001**, *34* (8), 2502−2511.

(12) Lu, Y.; Wang, Y. T.; Jiang, Z. Y.; Men, Y. F. Molecular Weight Dependency of Surface Free Energy of Native and Stabilized Crystallites in Isotactic Polypropylene. *ACS Macro Lett.* **2014**, *3* (11), 1101−1105.

(13) Wang, Y. T.; Lu, Y.; Jiang, Z. Y.; Men, Y. F. Molecular Weight Dependency of Crystallization Line, Recrystallization Line, and Melting Line of Polybutene-1. *Macromolecules* **2014**, *47* (18), 6401−6407.

(14) Luciani, L.; Seppala, J.; Lofgren, B. Poly-1-Butene - Its Preparation, Properties and Challenges. *Prog. Polym. Sci.* **1988**, *13* (1), 37−62.

(15) Miller, R. L.; Holland, V. F. On Transformations in Isotactic Polybutene-1. *J. Polym. Sci., Part B: Polym. Lett.* **1964**, *2* (5pb), 519−521.

(16) Boor, J.; Youngman, E. A. Polymorphism in Poly-1-Butene - Apparent Direct Formation of Modification I. *J. Polym. Sci., Part B: Polym. Lett.* **1964**, *2* (9pb), 903−907.

(17) Jones, A. T.; Aizlewood, J. M. Crystalline Forms of Polypentene-1. *J. Polym. Sci., Part B: Polym. Lett.* **1963**, *1* (9), 471−476.

(18) Wang, Y. T.; Liu, P. R.; Lu, Y.; Men, Y. F. Mechanism of Polymorph Selection during Crystallization of Random Butene-1/Ethylene Copolymer. *Chin. J. Polym. Sci.* **2016**, *34* (8), 1014−1020.

(19) Wang, Y. T.; Lu, Y.; Zhao, J. Y.; Jiang, Z. Y.; Men, Y. F. Direct Formation of Different Crystalline Forms in Butene-1/Ethylene Copolymer via Manipulating Melt Temperature. *Macromolecules* **2014**, *47* (24), 8653−8662.

(20) Jones, A. T. Polybutene-1 - Type II Crystalline Form. *J. Polym. Sci., Part B: Polym. Lett.* **1963**, *1* (8), 455−456.

DOI: 10.1021/acs.macromol.7b00771
Macromolecules 2017, 50, 5490−5497

(21) Natta, G.; Corradini, P.; Bassi, I. W. Crystal Structure of Isotactic Poly-alpha-Butene. *Nuovo Cimento* **1960**, *15*, 52−67.
(22) Boor, J.; Mitchell, J. C. Kinetics of Crystallization and a Crystal-Crystal Transition in Poly-1-Butene. *J. Polym. Sci., Part A: Gen. Pap.* **1963**, *1* (1), 59−84.
(23) Tashiro, K.; Asanaga, H.; Ishino, K.; Tazaki, R.; Kobayashi, M. Development of a New Software for the X-Ray Structural Analysis of Polymer Crystals by Utilizing the X-Ray Imaging Plate System. *J. Polym. Sci., Part B: Polym. Phys.* **1997**, *35* (11), 1677−1700.
(24) Tashiro, K.; Hu, J.; Wang, H.; Hanesaka, M.; Saiani, A. Refinement of the Crystal Structures of Forms I and II of Isotactic Polybutene-1 and a Proposal of Phase Transition Mechanism between Them. *Macromolecules* **2016**, *49* (4), 1392−1404.
(25) Tanaka, A.; Sugimoto, N.; Asada, T.; Onogi, S. Orientation and Crystal Transformation in Polybutene-1 under Stress Relaxation. *Polym. J.* **1975**, *7* (5), 529−537.
(26) Liu, Y.; Cui, K.; Tian, N.; Zhou, W.; Meng, L.; Li, L.; Ma, Z.; Wang, X. Stretch-Induced Crystal−Crystal Transition of Polybutene-1: An in Situ Synchrotron Radiation Wide-Angle X-ray Scattering Study. *Macromolecules* **2012**, *45* (6), 2764−2772.
(27) Chen, W.; Li, X. Y.; Li, H. L.; Su, F. M.; Zhou, W. M.; Li, L. B. Deformation-induced crystal-crystal transition of polybutene-1: an in situ FTIR imaging study. *J. Mater. Sci.* **2013**, *48* (14), 4925−4933.
(28) Cavallo, D.; Kanters, M. J. W.; Caelers, H. J. M.; Portale, G.; Govaert, L. E. Kinetics of the Polymorphic Transition in Isotactic Poly(1-butene) under Uniaxial Extension. New Insights From Designed Mechanical histories. *Macromolecules* **2014**, *47* (9), 3033−3040.
(29) Nakafuku, C.; Miyaki, T. Effect of Pressure on the Melting and Crystallization Behavior of Isotactic Polybutene-1. *Polymer* **1983**, *24* (2), 141−148.
(30) Li, L.; Liu, T.; Zhao, L.; Yuan, W. K. CO_2-Induced Crystal Phase Transition from Form II to I in Isotactic Poly-1-butene. *Macromolecules* **2009**, *42* (6), 2286−2290.
(31) Shi, J. Y.; Wu, P. Y.; Li, L.; Liu, T.; Zhao, L. Crystalline Transformation of Isotactic Polybutene-1 in Supercritical CO_2Studied by In-situ Fourier Transform Infrared Spectroscopy. *Polymer* **2009**, *50* (23), 5598−5604.
(32) Xu, Y.; Liu, T.; Li, L.; Li, D. C.; Yuan, W. K.; Zhao, L. Controlling Crystal Phase Transition from Form II to I in Isotactic Poly-1-butene Using CO_2. *Polymer* **2012**, *53* (26), 6102−6111.
(33) Shao, H. F.; Ma, Y. P.; Nie, H. R.; He, A. H. Solvent Vapor Annealing Induced Polymorphic Transformation of Polybutene-1. *Chin. J. Polym. Sci.* **2016**, *34* (9), 1141−1149.
(34) Jones, A. T. Cocrystallization in Copolymers of α-olefins II—Butene-1 Copolymers and Polybutene Type II/I Crystal Phase Transition. *Polymer* **1966**, *7* (1), 23−59.
(35) Qiao, Y. N.; Wang, Q.; Men, Y. F. Kinetics of Nucleation and Growth of Form II to I Polymorphic Transition in Polybutene-1 as Revealed by Stepwise Annealing. *Macromolecules* **2016**, *49* (14), 5126−5136.
(36) Powers, J.; Hoffman, J. D.; Weeks, J. J.; Quinn, F. A. Crystallization Kinetics and Polymorphic Transformations in Polybutene-1. *J. Res. Natl. Bur. Stand., Sect. A* **1965**, *69* (4), 335−345.
(37) Gohil, R. M.; Miles, M. J.; Petermann, J. On the Molecular Mechanism of the Crystal Transformation (Tetragonal-Hexagonal) in Polybutene-1. *J. Macromol. Sci., Part B: Phys.* **1982**, *21* (2), 189−201.
(38) Maruyama, M.; Sakamoto, Y.; Nozaki, K.; Yamamoto, T.; Kajioka, H.; Toda, A.; Yamada, K. Kinetic Study of the II-I Phase Transition of Isotactic Polybutene-1. *Polymer* **2010**, *51* (23), 5532−5538.
(39) Miller, R. L.; Nielsen, L. E. Crystallographic Data for Various Polymers. II. *J. Polym. Sci.* **1961**, *55* (162), 643−656.
(40) Brandrup, J.; Immergut, E. H.; Grulke, E. A. *Polymer Handbook*, 4th ed.; John Wiley & Sons: New York, 1999.
(41) Zeng, J.; Bian, F.; Wang, J.; Li, X.; Wang, Y.; Tian, F.; Zhou, P. Performance on absolute scattering intensity calibration and protein molecular weight determination at BL16B1, a dedicated SAXS beamline at SSRF. *J. Synchrotron Radiat.* **2017**, *24* (2), 509−520.
(42) Glatter, O.; Kratky, O. *Small-Angle X-ray Scattering*; Academic Press: London, 1982.
(43) Strobl, G. R.; Schneider, M. Direct Evaluation of the Electron-Density Correlation-Function of Partially Crystalline Polymers. *J. Polym. Sci., Polym. Phys. Ed.* **1980**, *18* (6), 1343−1359.
(44) Strobl, G. R.; Schneider, M. J.; Voigtmartin, I. G. Model of Partial Crystallization and Melting Derived from Small-Angle X-Ray-Scattering and Electron-Microscopic Studies on Low-Density Polyethylene. *J. Polym. Sci., Polym. Phys. Ed.* **1980**, *18* (6), 1361−1381.
(45) Alfonso, G. C.; Azzurri, F.; Castellano, M. Analysis of Calorimetric Curves Detected during the Polymorphic Transformation of Isotactic Polybutene-1. *J. Therm. Anal. Calorim.* **2001**, *66* (1), 197−207.
(46) Di Lorenzo, M. L.; Androsch, R.; Righetti, M. C. The Irreversible Form II to Form I Transformation in Random Butene-1/Ethylene Copolymers. *Eur. Polym. J.* **2015**, *67*, 264−273.
(47) Rubin, I. D. Relative Stabilities of Polymorphs of Polybutene-1 Obtained from the Melt. *J. Polym. Sci., Part B: Polym. Lett.* **1964**, *2*, 747−749.
(48) Fischer, E. W. Studies of Structure and Dynamics of Solid Polymers by Elastic and Inelastic Neutron-Scattering. *Pure Appl. Chem.* **1978**, *50*, 1319−1341.
(49) Tashiro, K.; Imanishi, K.; Izuchi, M.; Kobayashi, M.; Itoh, Y.; Imai, M.; Yamaguchi, Y.; Ohashi, M.; Stein, R. S. Cocrystallization and Phase Segregation of Polyethylene Blends between the D-Species and H-Species 0.8. Small-Angle Neutron-Scattering Study of the Molten State and the Structural Relationship of Chains between the Melt and the Crystalline State. *Macromolecules* **1995**, *28* (25), 8484−8490.
(50) Kaji, K. In *Applications of Neutron Scattering to Soft Condensed Matter*; Gabrys, B. J., Ed.; Gordon and Breach Science Publisher: New York, 2000; p 107.
(51) Cheng, S. Z. D. In *Phase Transitions in Polymers*; Elsevier: Amsterdam, 2008; Chapter 2, pp 17−59.
(52) Cheng, S. Z. D.; Noid, D. W.; Wunderlich, B. Molecular Segregation and Nucleation of Poly(Ethylene Oxide) Crystallized from the Melt 0.4. Computer Modeling. *J. Polym. Sci., Part B: Polym. Phys.* **1989**, *27* (5), 1149−1160.
(53) Miyoshi, T.; Mamun, A.; Reichert, D. Fast Dynamics and Conformations of Polymer in a Conformational Disordered Crystal Characterized by1H−13C WISE NMR. *Macromolecules* **2010**, *43* (8), 3986−3989.
(54) Miyoshi, T.; Mamun, A. Critical Roles of Molecular Dynamics in the Superior Mechanical Properties of Isotactic-Poly(1-butene) Elucidated by Solid-State NMR. *Polym. J.* **2012**, *44* (1), 65−71.

DOI: 10.1021/acs.macromol.7b00771
Macromolecules 2017, 50, 5490−5497